HHS Public Access

Author manuscript

Nat Cell Biol. Author manuscript; available in PMC 2018 September 26.

Published in final edited form as:

Nat Cell Biol. 2018 April ; 20(4): 455–464. doi:10.1038/s41556-018-0071-x.

L3MBTL2 orchestrates ubiquitin signaling by dictating the sequential recruitment of RNF8 and RNF168 after DNA damage

Somaira Nowsheen[1,2], **Khaled Aziz**[1], **Asef Aziz**[3], **Min Deng**[4], **Bo Qin**[2,4], **Kuntian Luo**[4], **Karthikbabu B Jeganathan**[3], **Henan Zhang**[5], **Tongzheng Liu**[4,6], **Jia Yu**[2], **Yibin Deng**[7], **Jian Yuan**[2,8], **Wei Ding**[5], **Jan M van Deursen**[3], and **Zhenkun Lou**[4,8,*]

[1]Mayo Medical Scientist Training Program, Mayo Clinic School of Medicine and Mayo Clinic Graduate School of Biomedical Sciences, Mayo Clinic, Rochester, MN 55905, USA

[2]Department of Molecular Pharmacology and Experimental Therapeutics, Mayo Clinic, Rochester, MN 55905, USA

[3]Department of Pediatrics and Adolescent Medicine, Mayo Clinic, Rochester, MN 55905, USA

[4]Department of Oncology, Mayo Clinic, Rochester, MN 55905, USA

[5]Department of Hematology, Mayo Clinic, Rochester, MN 55905, USA

[6]Jinan University, Institute of Tumor Pharmacology, Guangzhou, China

[7]Laboratory of Cancer Genetics, The University of Minnesota Hormel Institute, Austin, MN 55912, USA

[8]Research Center for Translational Medicine, East Hospital, Tongji University School of Medicine, Shanghai 200120, China

Abstract

Cells respond to cytotoxic DNA double strand breaks by recruiting DNA repair proteins to the damaged site. This recruitment is dependent on ubiquitylation of adjacent chromatin areas by E3 ubiquitin ligases such as RNF8 and RNF168. RNF8 and RNF168 are recruited sequentially to the double strand breaks. However, it is unclear what dictates the sequential order and recruits RNF168 to the DNA lesion. Here, we reveal that Lethal(3)malignant brain tumor-like protein 2 (L3MBTL2) is the missing link between RNF8 and RNF168. We found that L3MBTL2 is recruited by MDC1 and subsequently ubiquitylated by the E3 ligase RNF8. Ubiquitylated L3MBTL2, in turn, facilitates recruitment of RNF168 to the DNA lesion and promotes DNA double strand break repair. These results identify L3MBTL2 as a key target of RNF8 following

*Further information and requests for resources and reagents should be directed to and will be fulfilled by the corresponding author, Dr. Zhenkun Lou (lou.zhenkun@mayo.edu).

AUTHOR CONTRIBUTIONS

S.N., M.D., J.Y., and B.Q. designed and performed the experiments. K.J. and K.A. assisted with the telomere-fusion assay. K.A. and A.A. assisted with confocal microscopy. S.N. designed experiments, analyzed the data and wrote the manuscript with input from the other authors. Z.L. conceived and supervised the project.

COMPETING FINANCIAL INTERESTS

The authors declare no competing financial interests.

DNA damage and demonstrates how the DNA damage response pathway is orchestrated by ubiquitin signaling.

INTRODUCTION

Our genome is under constant threat, both from endogenous and exogenous agents. To preserve genomic integrity, cells have evolved an intricate system called the DNA damage response system, since a single unrepaired double strand break (DSB) can be lethal to the cell. This involves cell cycle arrest, transcriptional changes, DNA repair, and cell death in the event that the damage cannot be repaired[1]. In response to DSBs, cells recruit DNA repair proteins to the damaged site that extensively modify the adjacent chromatin[2]. Ubiquitin signaling plays an important role in coordinating the recruitment of DNA repair factors such as BRCA1 and 53BP1. Two critical factors in this early DNA damage signaling event are the RING-type ubiquitin E3 ligases RNF8 and RNF168[3, 4]. MDC1 recruits RNF8, which helps recruit RNF168. RNF168 then promotes the ubiquitination of histone H2A/H2AX, which is important for the recruitment of 53BP1 and BRCA1[3, 5–12]. However, how RNF8 promotes RNF168 recruitment was unclear, and an X factor was hypothesized to be a missing link between RNF8 and RNF168[13]. There has been considerable interest in the field in identifying this missing link (protein X).

Lethal(3)malignant brain tumor-like protein 2 (L3MBTL2), a putative polycomb group (PcG) protein, is essential for embryonic development and mutated in various malignancies[14–17]. It possesses transcriptional repression activity and is involved in chromatin compaction[17, 18]. This function is mediated by various complexes of proteins, such as E2F6 and PRC1 subcomplexes, of which L3MBTL2 is a subunit[15, 17, 19, 20]. L3MBTL2 possesses a zinc finger domain at the N-terminus and four centrally located MBT domains. These MBT domains recognize methylated histones[21]. Although another MBT domain containing protein, L3MBTL1, has been implicated in the DNA damage response pathway[22], there are no reports on any roles of L3MBTL2 in DNA damage response. In addition, mutations in L3MBTL2 are prevalent in various cancers including leukemia, a disease characterized by alterations in multiple DNA repair proteins. For these reasons we wanted to explore the role of L3MBTL2 in the DNA damage response pathway. Here, we reveal that L3MBTL2 is the missing link between RNF8 and RNF168.

RESULTS

L3MBTL2 plays a role in DNA damage response and is an ATM substrate

In order to test whether L3MBTL2 has a role in DNA damage response, we utilized a reporter system in U2OS cells[23] to induce one DSB per cell by I-SceI to examine the localization of L3MBTL2. Upon induction of a DSB, we found that L3MBTL2 localized to the site of damage (Figures 1a–b), suggesting that it has a possible role in DNA damage response. L3MBTL2 also formed ionizing radiation-induced foci that overlapped with γ-H2AX[24] (Figures 1c–d). We further found that L3MBTL2 is phosphorylated at ATM/ATR consensus motifs in an ATM-dependent manner (Figure 1e). Analysis of L3MBTL2 protein sequence revealed two potential ATM-phosphorylation consensus sequences, S158 and S335

(Figure 1f). By mutating these putative ATM phosphorylation sites on L3MBTL2 individually or in combination, we found that S335 of L3MBTL2 is phosphorylated following DNA damage (Figure 1g). We next tested whether L3MBTL2 phosphorylation affects its localization following DNA damage. As shown in Figures 1h–j, wild-type L3MBTL2 formed foci following exposure to irradiation (IR) while the phosphorylation mutant showed diffuse nuclear staining, suggesting that phosphorylation by ATM at S335 is required for the localization of L3MBTL2 to DNA damage sites.

ATM-mediated phosphorylation of L3MBTL2 promotes its interaction with MDC1 and recruits it to double strand breaks

We next investigated the mechanism of recruitment of L3MBTL2 to the DSB. We found that depletion of MDC1, an upstream mediator protein in the DNA damage response[6, 7, 25], abolished L3MBTL2 localization to the DSB (Figures 2a–c). In addition, co-immunoprecipitation (co-IP) experiments revealed that MDC1 and L3MBTL2 interact following DNA damage (Figure 2d). This led us to test whether the interaction between MDC1 and L3MBTL2 was phosphorylation dependent. Indeed, the S335A mutant failed to interact with MDC1 in co-IP experiments (Figure 2e). Thus, ATM-mediated phosphorylation of L3MBTL2 promotes its interaction with MDC1 and recruits it to DSBs.

MDC1 contains tandem BRCT domains and a FHA domain that recognize phosphorylated serine/threonine (pS/T) containing motifs[4, 26, 27]. We found that the MDC1-L3MBTL2 interaction was dependent on the FHA, but not BRCT domain of MDC1 both by co-IP and GST-pull down assays (Figures 2f–h). Furthermore, the phosphorylation mutant of L3MBTL2 was unable to interact with the FHA domain of MDC1 (Figure 2i). Using GST-tagged FHA protein and either non phosphorylated or phosphorylated L3MBTL2 peptides, we validated that this binding between L3MBTL2 and MDC1 is, in fact, a direct interaction (Figure 2j). These results were verified with the MDC1 FHA mutant R58A that disrupts the binding between the FHA domain and its partners[28, 29] (Figures 2k–m). The specificity of the L3MBTL2 antibody was verified by western blot and immunofluorescence (Supplementary Figures 1a–b). Collectively, these results establish that the FHA domain of MDC1 and phosphorylated S335 of L3MBTL2 mediate their interaction.

L3MBTL2 recruits RNF168 to double strand breaks

Next, we sought to determine the functional role of L3MBTL2 in mediating a robust DNA damage response. The response to DSBs involves ATM activation and ensuing phosphorylation of γ-H2AX, which binds directly to and recruits MDC1[30, 31]. RNF8 and RNF168 are then recruited sequentially at this step in the DNA damage response pathway in an MDC1-dependent manner[3, 4, 32]. To understand the role of L3MBTL2 in DNA damage response, we knocked down endogenous L3MBTL2 using shRNAs and probed various DNA damage response proteins. L3MBTL2 did not affect the recruitment of MDC1 or RNF8 to DSBs (Figures 3a–c). Intriguingly, knockdown of L3MBTL2 abolished the localization of RNF168 to damage sites, suggesting L3MBTL2 plays a role in its recruitment (Figures 3a–c). Furthermore, in cells depleted of endogenous L3MBTL2 and reconstituted with WT or S335A L3MBTL2, we found that WT, but not the S335A mutant could rescue RNF168 foci (Figures 3d–f). Since L3MBTL2 is a PcG, we wondered if the effects observed with

L3MBTL2 knockdown were due to transcriptional effect and subsequent changes in RNF168 protein levels. However, we did not observe any significant alterations in RNF168 protein levels at the time points studied (Figure 3c). The levels of other regulators of RNF168, such as MDC1, RNF8, and UBC13 were also not affected (Figure 3c and Supplementary Figures 4b–c). In addition, we tested whether other PcG members, G9A, E2F6, or PCGF6 are able to regulate RNF168 foci. We did not observe any difference in RNF168 recruitment to DSBs following G9A knockdown (Supplementary Figures 2a–c), E2F6 knockdown (Supplementary Figures 2d–f) or PCGF6 knockdown (Supplementary Figures 2g–i). Previously, another member of the L3MBT family, L3MBTL1, was reported to be involved in DNA DSB repair[22, 33]. To elucidate if the effects observed were specific to L3MBTL2, we knocked down endogenous L3MBTL1 in U2OS cells using shRNAs and probed for RNF168 foci. We did not observe any significant differences in RNF168 foci in control vs knockdown cells (Supplementary Figures 2j–l). Collectively, these results suggest that the role of L3MBTL2 in RNF168 regulation is distinct from other family member or its role in epigenetic regulation.

To understand the molecular basis of these observations, we performed co-immunoprecipitation experiments to look at interacting partners of L3MBTL2. Interestingly, both RNF8 and RNF168 were pulled down with endogenous L3MBTL2 following DNA damage (Figure 3g and Supplementary Figure 2m–n). Furthermore, the RNF168-L3MBTL2 interaction, but not MDC1-L3MBTL2 interaction, was dependent on RNF8 (Figure 3h and Supplementary Figure 2o). In contrast, knockdown of RNF168 did not affect the interaction between RNF8 and L3MBTL2 (Supplementary Figure 2n). The results were validated with the FHA mutant of MDC1 and phosphorylation mutant of L3MBTL2 (Supplementary Figures 2p–q). In addition, formation of radiation-induced L3MBTL2 foci was independent of RNF8 (Supplementary Figures 2r–t). Taken together, our data suggests that L3MBTL2 interacts with RNF168 in a RNF8 dependent manner and regulates RNF168 foci formation. This is very similar to the protein X proposed to recruit RNF168[13] and led us to hypothesize that L3MBTL2 is a key RNF8 substrate that provides an initial binding platform for RNF168 following DNA damage.

RNF8 mediated K63 linked ubiquitylation of L3MBTL2 following DNA damage is critical for the interaction with UDM1 of RNF168 and subsequent histone ubiquitylation

To test our hypothesis that L3MBTL2 is the key RNF8 substrate that recruits RNF168 to DSBs, we determined whether L3MBTL2 is an obligate substrate of RNF8. To test this, we examined L3MBTL2 ubiquitylation before and after DNA damage. We observed robust ubiquitylation of L3MBTL2 following DNA damage (Figure 4a). Knockdown of RNF8 greatly reduced the ubiquitylation of L3MBTL2, suggesting that L3MBTL2 is ubiquitylated in a RNF8-dependent manner (Figure 4a and Supplementary Figure 3a). Similar defects in L3MBTL2 ubiquitylation was observed with the S335A mutant that is unable to localize to the DSB and in MDC1-depleted cells (Supplementary Figures 3b–c), suggesting the ubiquitylation of L3MBTL2 occurs at the sites of DNA damage. When we examined the linkage of L3MBTL2 ubiquitylation, we found that L3MBTL2 was mainly ubiquitylated through K63-specific chains, which are predominantly involved in recruiting proteins to DSB sites[34] (Figure 4b). To check whether a direct interaction with RNF8 is required for

DNA damage induced K63-linked polyubiquitylation of L3MBTL2, we utilized bacterially expressed recombinant proteins. Based on published literature, we utilized Ubc13/Ube2V as the E2 conjugating enzyme[11]. Again, we observed polyubiquitylation of L3MBTL2 only in the presence of RNF8 (E3) *in vitro* (Figure 4c). These results suggest that RNF8 directly regulates K63-linked ubiquitin chain formation on L3MBTL2.

To further characterize how RNF8 and L3MBTL2 couple ubiquitin dependent DSB signaling in the accrual of RNF168 to DSBs, we utilized recombinant Ub-binding domains of RNF168[35]. The reaction mixture from Figure 4c was incubated with RNF168 wild-type (WT), UDM1 or UDM2 proteins immobilized on GST beads in the presence or absence of the E3 ligase, RNF8. Interestingly, ubiquitylated L3MBTL2 only bound to the UDM1 domain of RNF168 (Figure 4d). This is consistent with the previous report that UDM1 domain of RNF168 is important for its recruitment[5, 36]. As a test of specificity, we mutated sites on RNF168 that have previously been reported to be important for its association with RNF8-mediated K63-linked ubiquitin products[3, 13, 37]. Indeed, mutation of these sites reduced the interaction between L3MBTL2 and UDM1 (Figure 4e). Furthermore, in accordance with previous reports, UDM1 was only able to recognize K63-linked ubiquitin linkages (Figure 4f). These results suggest that RNF8-ubiquitylated L3MBTL2 directly interacts with UDM1 domain of RNF168 via K63-linked ubiquitin chains.

While this manuscript was in preparation, Thorslund, et al reported that histone H1 undergoes K63-linked polyubiquitylation by RNF8 which then anchors RNF168 onto DSBs[38]. Contrary to their report, we did not observe any significant alterations in RNF168 accrual to DSBs following histone H1 knockdown using the same cocktail of siRNAs and same cell line that they utilized (Supplementary Figures 3d–f). In a direct comparison between L3MBTL2 knockout and histone H1 knockdown, only L3MBTL2 consistently reduced BRCA1 and 53BP1 foci formation (Supplementary Figures 3g–i). We also did not observe any changes in H2A K15 ubiquitylation with histone H1 knockdown (Supplementary Figure 3h). Moreover, Thorslund, et al., utilized the high-mobility group protein HMGB1 that nonspecifically competes with histone H1 for chromatin binding to suppress RNF168 foci. However, we did not observe any alterations in RNF168 foci formation using the same protocol (Supplementary Figures 3j–l). Finally, the authors reported that RNF8-mediates K63 linked polyubiquitylation of histone H1 following DNA damage as part of the DNA damage response. However, we did not have the same observations and, in fact, see a single band the same molecular weight as monoubiquitylated histone H1, and upon the deubiquitinase USP2 treatment, shifted down to the size of unmodified histone H1, suggesting histone H1 undergoes monoubiquitylation following DNA damage induction (Supplementary Figure 3m). No interaction between histone H1 and UDM1 was observed as well (Supplementary Figure 3n). Using the same K63 Super UIM pull down approach and the same histone H1.x antibody, we were unable to detect any histone H1 ubiquitylation even though a robust L3MBTL2 ubiquitylation was detected (Supplementary Figure 3o). Other reports also failed to observe histone H1 polyubiquitylation[35, 39]. Together, these results raise the question whether, indeed, histone H1 couples the ubiquitin signaling after DNA damage. We also tested whether histone H1 and L3MBTL2 interact to mediate the effect observed. However, we did not observe any interaction between L3MBTL2 and histone H1 (Supplementary Figure 3p). Taken together,

our data demonstrates that L3MBTL2, rather than histone H1, links the aforementioned signaling pathway.

DNA damage induced RNF8 mediated ubiquitylation of L3MBTL2 is critical for DNA DSB repair

To reveal the mechanism underlying RNF168 recruitment to DSBs by L3MBTL2, we mapped the residue on L3MBTL2 that is ubiquitylated by RNF8. We used the publicly available database PhosphoSite[40] to identify possible ubiquitylation sites. We mutated candidate lysines and found that mutation at lysine 659 (K659) abolished L3MBTL2 ubiquitylation following DNA damage, suggesting that K659 was the site of RNF8-mediated ubiquitylation (Figure 5a). Moreover, wild-type L3MBTL2, but not the K659R mutant, was able to be ubiquitylated by RNF8 *in vitro* (Figure 5b). The mutation at K659 also affected the recognition of ubiquitin chain of L3MBTL2 by the UDM1 domain of RNF168 both in cells and *in vitro* (Figures 5b–c). Importantly, the ubiquitylation mutation abolished the binding between RNF168 and L3MBTL2 without affecting the MDC1-L3MBTL2 interaction in cells (Figure 5d). These results suggest that RNF8-mediated ubiquitylation of L3MBTL2 at K659 is critical for the RNF168-L3MBTL2 interaction.

To assess if ubiquitylation of L3MBTL2 affects the function of RNF168 in DNA damage response, we utilized L3MBTL2 knockout U2OS cells. We reconstituted WT or K659R mutant and exposed the cells to IR to induce DNA damage. While the K659R mutant was able to form L3MBTL2 foci, the K659R mutation compromised RNF168 foci formation (Figure 5e and Supplementary Figure 4a). The recruitment of DNA repair proteins upstream of RNF168 such as γ-H2AX and RNF8 was unaffected by K659R mutation. However, recruitment of downstream proteins such as BRCA1 and 53BP1 was hampered (Figure 5e and Supplementary Figure 4a). Moreover, expression of the K659R mutation did not alter the protein levels of key DNA repair proteins, such as DNA-PK, MDC1, RNF8, RNF168, BRCA1, and UBC13 (Supplementary Figures 4b–c). It has been reported that RNF168 catalyzes histone H2A ubiquitylation at K13/15 to facilitate the recruitment of downstream factors[13]. We examined H2AK15 ubiquitylation using a specific antibody recognizing H2A K15 Ub[41]. Consistent with RNF8 and RNF168 knockdown results that have been reported, L3MBTL2 knockout suppressed DSB-induced H2A ubiquitylation (Figure 5f). Re-expression of WT L3MBTL2 rescued H2A ubiquitylation while reconstitution of the K659R or S335A mutant failed to do so (Figure 5f). Taken together, our results support the notion that RNF8-mediated K63-linked polyubiquitylation of L3MBTL2 underlies RNF168 recruitment to DSBs by facilitating the interaction between ubiquitylated L3MBTL2 and the UDM1 domain of RNF168 and enables recruitment of downstream repair proteins.

If our hypothesis that L3MBTL2 is a critical DNA DSB repair protein is true, we expect the L3MBTL2 knockout cells to be sensitive to radiation. To test this hypothesis, we knocked out endogenous L3MBTL2 in MDA-MB-231 breast cancer cells and subsequently exposed them to IR. Indeed, L3MBTL2 deficient MDA-MB-231 cells were more sensitive to radiation compared to parental cells (Figure 5g and Supplementary Figure 4d), suggesting that L3MBTL2 does, in fact, play a role in DNA damage response. Loss of RNF168 alone or together with L3MBTL2 sensitized the cells to IR to a similar extent, suggesting that

L3MBTL2 and RNF168 are in the same pathway. Expression of wild-type (WT) L3MBTL2 conferred radioresistance while the K659R mutant was sensitive to IR (Supplementary Figures 4e–f). Similar results were observed with U2OS cells suggesting that the radiosensitivity observed with loss of L3MBTL2 is independent of p53 status (Supplementary Figures 4g–h). These results offer a potential therapeutic option for cancers with mutations in L3MBTL2. Finally, global reduction in ubiquitin irradiation-induced foci was observed with L3MBTL2 deficiency suggesting that L3MBTL2 is a key player in this pathway (Supplementary Figures 4i–j).

We also sought to identify the domain(s) of L3MBTL2 responsible for the effects observed. Each domain of L3MBTL2 was deleted individually and the effect of the deletion on RNF168 foci formation was assessed. As shown in Supplementary Figures 4k–l, deletion of any of the four MBT domains abolished radiation-induced RNF168 foci formation. This is most likely due to disruption of the protein structure. Further research is warranted in this avenue to decipher the role of these domains on DNA damage response.

L3MBTL2 regulates class switch recombination and chromosome end fusions

Given that RNF8 and RNF168 ubiquitin ligases are essential for class switch recombination[42] and telomere-telomere fusions after loss of TRF2[43], we assessed the effect of L3MBTL2 knockdown on these processes. As shown in Figures 6a–d, knockdown of L3MBTL2 abrogated both processes. Epistasis between RNF8-L3MBTL2 and RNF168-L3MBTL2 was also observed, further suggesting that these proteins are in the same pathway. Taken together, our results indicate that L3MBTL2 mediates RNF8-RNF168 signaling and is important for DNA DSB repair and physiological processes.

DISCUSSION

Aberrations in DNA damage response signaling cascade can lead to diseases such as cancer. Ubiquitin modification plays a key role in DNA damage response thus identifying critical players in this pathway is important for advancing the field. In this study, we propose that L3MBTL2 is the missing link between the E3 ubiquitin ligases, RNF8 and RNF168, and explain how RNF168 UDMs impart such high-level specificity for their respective targets. This is also the first report to our knowledge linking L3MBTL2 to DNA damage response. Our findings suggest a model by which sequential phosphorylation by ATM and subsequent recruitment of L3MBTL2 to DSB sites allow RNF8-mediated K63-linked ubiquitylation of L3MBTL2 to promote ubiquitin-dependent protein recruitment, i.e. the recruitment of RNF168, to sites of DNA DSBs. RNF168 subsequently ubiquitylates proteins such as histone H2A to trigger recruitment of additional DSB repair proteins such as 53BP1 and BRCA1 to promote DSB repair (Figure 6e).

While this project was in progress, it was reported that histone H1 is the key signaling intermediate between RNF8 and RNF168[38]. We tried to determine how histone H1 plays into our observations with L3MBTL2. However, we were unable to reproduce their observations using the same reagents and cell lines (Supplementary Figure 3). We knocked down histone H1 with RNAi but were unable to observe the defect in histone H2A ubiquitylation or the assembly of RNF168 and its downstream factors at DSBs. The

knockdown efficiency achieved by our group seems to be comparable to what was reported in the previous report, although we cannot completely exclude the possibility that the discrepancy might be caused by a difference in knockdown efficiency of histone H1. Over the last few decades, other groups have studied histone H1 ubiquitylation, and like us, have only observed monoubiquitylation of this histone[35, 39]. In addition histone H1 has been observed to move away from the DSB site[44]. This decreases the likelihood that histone H1 is the platform for RNF168 recruitment. Together, these results support of a key role of L3MBTL2 as signaling intermediate in the ubiquitin-driven DSB signal transduction cascade.

In conclusion, our findings challenge the current model that histone H1 is the major linker between RNF8 and RNF168 for H2A and H2AX ubiquitylation during DNA DSB repair[38]. We suggest that L3MBTL2 is the missing link between RNF8 and RNF168 (Figure 6e). Therapeutically, L3MBTL2 mutation in cancer patients might enhance the efficacy of DNA damaging agents.

METHODS

Cell culture

HEK293, HEK293T, U2OS and MDA-MB-231 cell lines were purchased from ATCC. CH12F3-2a cells were purchased from Thermo Fisher Scientific. The identities of all cell lines were confirmed by the Medical Genome facility at Mayo Clinic Center (Rochester, MN) using short tandem repeat profiling upon receipt. The cell lines were maintained in DMEM, McCoy's 5A and RPMI1640 with 10% FBS respectively. U2OS I-SceI cells were generously provided by Dr. Maria Jasin (Memorial Sloan Kettering Cancer Center, NY) and maintained in McCoy's 5A supplemented with 10% FBS. SV40 transformed $TRF2^{F/F}$ MEFs were maintained as described previously[45].

Chemicals

Triamcinolone acetonide and the ATM inhibitor KU55933 (Sigma) were used in this study. KaryoMAX® Colcemid was purchased from Thermo Fisher Scientific.

Plasmids

Flag L3MBTL2 (Plasmid # 28232, provided by Dr. Danny Reinberg), lentiCRISPR v2 (Plasmid # 52961, provided by Dr. Feng Zhang) and Flag HMGB1 plasmids (Plasmid #31609, provided by Dr. Yasuhiko Kawakami) were purchased from Addgene. Flag L3MBTL2 was subcloned into pGEX-4T-2 vector (Clontech) and peGFP. L3MBTL2 S135A, L3MBTL2 S335A, L3MBTL2 S135/335A, and L3MBTL2 K659R mutants were generated by site-directed mutagenesis (Stratagene). The MDC1 plasmids have been described previously[7, 25, 31, 46]. Dr. Xiaochun Yu (City of Hope, CA) provided the plasmids expressing RNF8 and RNF168. RNF168 UDM1 (amino acids 110–201) and UDM2 (amino acids 419–487) fragments were amplified by PCR and inserted into pGEX4T2 (GE Lifesciences) for expression in *Escherichia coli*. Mutants of UDM1 were generated by site directed mutagenesis. His-tagged WT Ub, K63Ub (ubiquitin with all lysines other than lysine 63 mutated) and K63R Ub (ubiquitin with only lysine 63 mutated) have been

previously described[47]. Dr. Niels Mailand (University of Copenhagen) provided the K63 super UIM. Dr. Jan van Deursen generously provided the Cre lentiviral plasmid[48].

siRNA and shRNA knockdown, CRISPR knockout and peptides

siRNA sequences used in this study were as follows. Non-targeting control (#1) 5′-GGGAUACCUAGACGUUCUATT-3′; control (#2) 5'-UUCAAUAAAUUCUUGAGGUdTdT-3'; MDC1 (#1) 5'-UCCAGUGAAUCCUUGAGGUdTdT-3'; MDC1 (#2) 5'-ACAACAUGCAGAGAUUGAAdTdT-3'; histone H1 pooled from: H1 (#1) 5′-GCUACGACGUGGAGAAGAATT-3′; H1 (#4) 5′-CCUUUAAACUCAACAAGAATT-3′; H1 (#5) 5′-CCUUCAAACUCAACAAGAATT-3′; H1 (#9) 5′-CAGUGAAACCCAAAGCAAATT-3′; H1 (#10) 5′-CCUUCAAGCUCAACCGCAATT-3′; L3MBTL2 [ON-TARGET plus Human L3MBTL2 (83746) siRNA]. Two consecutive rounds of H1 siRNA cocktail transfection (with 24 h intervals at 30nM each) was performed in order to achieve as robust H1 knockdown as possible. shRNAs used in this study were as follows: L3MBTL2 (NM_031488, Sigma), L3MBTL1 (NM_015478, Sigma) RNF8 (Hs_RNF8, Open Biosystems), RNF168 (Hs_RNF168, Open Biosystems), G9A (NM_025256, Sigma), and E2F6 (NM_198256, Sigma), PCGF6 (NM_032154), RNF8 (mouse, NM_021419), RNF168 (mouse, NM_027355) and L3MBTL2 (mouse, NM_145993). Lentiviruses for infection of cells was performed as described previously[47]. Lentiviruses for infection of cells were packaged in HEK293T cells using Lipofectamine 2000 transfection reagent. 48 hours after transfection, medium was collected and added to the target cells with 8ug/mL polybrene to enhance infection efficiency. L3MBTL2 and MDC1 CRISPR plasmids were generated using the methods described previously[49]. The following guides were used: L3MBTL2: GGAGAAGCCCCGGAGTATTGAGG and GCTGCCTGGTCTGCCAAAATTGG; MDC1: GGTGTAACGTGGAGCCAGTAGGG and GGCCTACCACATTCTTCCCGAGG. The following peptides were synthesized and used in this manuscript: EVVDK{PSER}QVSRTRMAVVDT{LYS(BIOTIN)} and EVVDKSQVSRTRMAVVDT{LYS(BIOTIN)} (GenScript).

Denaturing Ni-NTA pulldown

Transiently transfected or virus infected cells were harvested and pellets were washed once in PBS. Cells were lysed in lysis buffer composed of 8M Urea, 0.1M NaH_2PO_4, 30 mM NaCl and 0.01M Tris (pH 8.0). Lysates were briefly sonicated to shear DNA and incubated with Ni-NTA agarose beads (QIAGEN) for 1–2 hours at room temperature. Beads were washed 5 times with a solution composed of 8M Urea, 0.1M NaH_2PO_4, 300mM NaCl and 0.01M Tris (pH 8.0). Input and beads were boiled in loading buffer and subjected to SDS-PAGE and immunoblotting.

Denaturing immunoprecipitation for ubiquitylation

The cells were lysed in 100μl lysis buffer composed of 62.5mM Tris-HCl (pH 6.8), 2% SDS, 10% glycerol, 20mM NEM and 1 mM iodoacetamide, boiled for 15 minutes, diluted 10 times with NETN buffer containing protease inhibitors, 20mM NEM and 1mM iodoacetamide and centrifuged to remove cell debris. The cell extracts were subjected to immunoprecipitation with the indicated antibodies, and blotted as indicated.

Immunoprecipitation, immunoblotting, and *in vitro* pull-down assay

We prepared cell lysates, performed immunoprecipitation, and immunoblotting as previously described[47]. Briefly, cells were lysed with NETN buffer (20mM Tris-HCl, pH 8.0, 100mM NaCl, 1mM EDTA, 0.5% Nonidet P-40) containing 50mM β-glycerophosphate, 10mM NaF, and 1 mg/ml each of pepstatin A and aprotinin. Whole cell lysates were centrifuged at 12000 rpm for 15 minutes. Whole cell lysates were incubated with 2μg of antibody and protein A or protein G Sepharose beads (Amersham Biosciences) for 2 hours or overnight at 4°C. The immunocomplexes were then washed with NETN buffer and separated by SDS–PAGE. Immunoblotting was performed following standard procedures. GST fusion proteins were bound to glutathione Sepharose for 3 hours at 4°C. The beads were washed with PBS twice and incubated with indicated proteins for 1 hour at 4°C. After washing with NETN, the bound proteins were separated by SDS-PAGE and immunoblotted with the indicated antibodies. Please refer to the **Reporting Summary** and Supplementary Table 2 for information of antibodies used.

Recombinant protein production

Purified proteins were obtained by expressing the proteins in an *Escherichia coli* strain *BL21* or commercially. Bacteria were grown in LB medium, induced with 0.25mM isopropyl-β-D-thiogalactoside (IPTG) for 2 hours at 37°C, and cultured at 16°C for 12 hours. The cells were then lysed using appropriate lysis buffer supplemented with Protease Inhibitor Cocktail (Roche). The proteins were purified by binding to appropriate beads for 3 hours at 4°C. The beads were washed with lysis buffer twice and the protein was subsequently eluted. Recombinant human UBA1, UBE2D3/UBCH5C, UBE2N/UBE2V2 complex, UBE2N (UBC13)/UEV1A complex, USP2, RNF8, RNF168, L3MBTL2, and ubiquitin (wild-type and mutants) used for *in vitro* ubiquitylation assays were purchased from Boston Biochem, Biotechne, Abnova and Origene.

Ubiquitylation and deubiquitylation assays

In vitro and *in vivo* ubiquitylation and deubiquitylation assays were performed as previously described[47]. Briefly, substrates were incubated at 30 °C in buffer containing 25mM Tris HCl, pH 7.4, 2mM ATP, 5mM $MgCl_2$, 5mM $MnCl_2$ and 0.1mM DTT for 1 hour for ubiquitylation. Deubiquitylation was performed in deubiquitylation buffer (50mM Tris-HCl pH 8.0, 50mM NaCl, 1mM EDTA, 10mM DTT, 5% glycerol) overnight at 16°C. Successive ubiquitylation and deubiquitylation was performed by purifying the ubiquitylated product by immunoprecipitation, washing the beads thoroughly, and then performing the deubiquitylation assay. The product was processed by boiling the sample with Laemmli buffer and performing SDS PAGE.

Immunofluorescence

To visualize ionizing radiation induced foci (IRIF), cells were cultured on coverslips and treated with 2Gy IR followed by recovery for 1 hour. Depending on the foci to be stained, cells were then washed in PBS, pre-extracted with a solution of 20mM Hepes pH 7.4, 50mM NaCl, 3mM $MgCl_2$, 300mM Sucrose, and 0.5% Triton-X for 10 minutes at room temperature, incubated in 3% paraformaldehyde for 15 minutes, and permeabilized in 0.5%

Triton solution for 5 minutes at room temperature. For others, incubation at −20°C in a 1:1 mixture of acetone: methanol was used as fixative. Samples were blocked with 5% goat serum and then incubated with primary antibody for 30 minutes. Samples were washed three times and incubated with secondary antibody for 30 minutes. Cells were stained with DAPI to visualize nuclear DNA. The coverslips were mounted onto glass slides with anti-fade solution and visualized using a Nikon eclipse 80i fluorescence microscope or laser scanning microscope (Zeiss LSM 880). >200 cells were counted per experiment. Please refer to the **Reporting Summary** and Supplementary Table 2 for information of antibodies used.

Colony formation assay

500–5000 cells were plated in triplicate in each well of 6 well plates. 16 hours later, cells were exposed to ionizing radiation, and left for 10–14 days at 37°C to allow colony formation. Colonies were stained with methylene blue and counted. Results were normalized to plating efficiencies.

Irradiation

Cells were irradiated with 2GY for immunofluorescence studies and 10GY for western blot/co-immunoprecipitation assays. Typically, cells were processed an hour after irradiation unless noted otherwise.

Class switch recombination

Class switch recombination was performed in CH12F3-2a cells as described previously[50]. Briefly, RNF8, RNF168, L3MBTL2 or a combination of these, was knocked down using shRNAs. 40 hours later, cells were stimulated with ligands [1 ng/ml of recombinant human TGF-β1 (R&D Systems), 10 ng/ml of recombinant murine IL-4 (R&D Systems), and 250 ng/ml recombinant murine CD40 ligand (PerproTech)]. For analyzing class switch from IgM (IgM+/IgA−) to IgA (IgM−/IgA+), CH12F3-2 cells were collected after 60 hours, intracellularly stained with PE-conjugated anti-murine IgA antibody (clone 11–44-2, eBiosciences, Cat# 12-5994-82). Membrane IgM expression was assessed using FITC-conjugated anti-murine IgM antibody (eBiosciences; Cat# 11-5890-82). Cytofix/Cytoperm and Perm/Wash buffers (BD Biosciences, catalog # 554714) was utilized. Cells were then analyzed on a FACS Calibur (BD Biosciences) at the Mayo Clinic Flow Cytometry Core. Data was analyzed using FlowJo software (TreeStar).

Telomere fusion assay

The assay was performed as described previously with slight modification[51]. Briefly, RNF8, RNF168, L3MBTL2 or a combination of these, was knocked down in $TRF2^{F/F}$ MEFs using shRNAs. 40 hours later, cells were infected with lenti-Cre. 96 hours after infection, cells were treated with KaryoMAX Colcemid (0.5μg/mL) for 5 hours. All cells including detached cells were harvested, incubated for 12 min at 37°C in 0.075 M KCl, and fixed in freshly prepared methanol:glacial acidic acid (3:1 vol/vol). Cells were stored at 4°C and when needed dropped onto wet slides and air-dried. PNA FISH was performed by the Mayo Clinic Cytogenetics Core using the Telomere PNA FISH kit (catalog# K532611-8, Agilent) following manufacturer's instructions. Images were acquired using fluorescent microscope.

Statistics and reproducibility

Data in bar and line graphs are presented as mean ± SEM of at least three independent experiments. >200 cells were counted per experiment for Figures 1b, 1d, 1i, 2c, 3a, 3d, 5e, and Supplemental Figures 2b, 2e, 2h, 2k, 2s, 3k, 4d, 4i, 4k. Statistical analyses were performed with ANOVA (GraphPad Prism). Statistical significance is represented in figures by: *, $p<0.05$; **, $p<0.01$. All western blot assays shown here were successfully repeated at least three times.

Data Availability

Source data for Figures 1–6 and Supplementary Figures 1–4 are provided in Supplementary Table 1. All data supporting the findings of this study are available from the corresponding author on reasonable request.

Supplementary Material

Refer to Web version on PubMed Central for supplementary material.

Acknowledgments

We thank Drs. Z. Zhang, M. Jasin, X. Yu, D. Reinberg, N. Dantuma, and N. Mailand for providing reagents. Thank you to the members of the Lou lab for helpful discussions and Dr. B. Davies for technical assistance. This work was supported, in part, by NIH grants CA130996, CA108961, and CA148940 (to Z.L.) and CA160333 (to Y.D.). S.N. was supported by the Laura J. Siegel Breast Cancer Fellowship Award from the Foundation for Women's Wellness. K.A. and S.N. thanks the Mayo Clinic MSTP for fostering an outstanding environment for physician-scientist training. We thank the Mayo Clinic Cancer Center for the use of the Cytogenetics Core, which provided PNA FISH services. Mayo Clinic Cancer Center is supported in part by an NCI Cancer Center Support Grant 5P30 CA15083-36.

References

1. Jackson SP, Bartek J. The DNA-damage response in human biology and disease. Nature. 2009; 461:1071–1078. [PubMed: 19847258]
2. Price Brendan D, D'Andrea Alan D. Chromatin Remodeling at DNA Double-Strand Breaks. Cell. 2013; 152:1344–1354. [PubMed: 23498941]
3. Doil C, et al. RNF168 Binds and Amplifies Ubiquitin Conjugates on Damaged Chromosomes to Allow Accumulation of Repair Proteins. Cell. 2009; 136:435–446. [PubMed: 19203579]
4. Kolas NK, et al. Orchestration of the DNA-damage response by the RNF8 ubiquitin ligase. Science (New York, N.Y.). 2007; 318:1637–1640.
5. Stewart GS, et al. The RIDDLE Syndrome Protein Mediates a Ubiquitin-Dependent Signaling Cascade at Sites of DNA Damage. Cell. 2009; 136:420–434. [PubMed: 19203578]
6. Goldberg M, et al. MDC1 is required for the intra-S-phase DNA damage checkpoint. Nature. 2003; 421:952–956. [PubMed: 12607003]
7. Stewart GS, Wang B, Bignell CR, Taylor AMR, Elledge SJ. MDC1 is a mediator of the mammalian DNA damage checkpoint. Nature. 2003; 421:961–966. [PubMed: 12607005]
8. Huen MS, et al. RNF8 transduces the DNA-damage signal via histone ubiquitylation and checkpoint protein assembly. Cell. 2007; 131:901–914. [PubMed: 18001825]
9. Kolas NK, et al. Orchestration of the DNA-damage response by the RNF8 ubiquitin ligase. Science. 2007; 318:1637–1640. [PubMed: 18006705]
10. Mailand N, et al. RNF8 ubiquitylates histones at DNA double-strand breaks and promotes assembly of repair proteins. Cell. 2007; 131:887–900. [PubMed: 18001824]

11. Wang B, Elledge SJ. Ubc13/Rnf8 ubiquitin ligases control foci formation of the Rap80/Abraxas/Brca1/Brcc36 complex in response to DNA damage. Proc Natl Acad Sci U S A. 2007; 104:20759–20763. [PubMed: 18077395]
12. Sobhian B, et al. RAP80 targets BRCA1 to specific ubiquitin structures at DNA damage sites. Science. 2007; 316:1198–1202. [PubMed: 17525341]
13. Mattiroli F, et al. RNF168 ubiquitinates K13-15 on H2A/H2AX to drive DNA damage signaling. Cell. 2012; 150:1182–1195. [PubMed: 22980979]
14. Khan FH, et al. Acquired genetic alterations in tumor cells dictate the development of high-risk neuroblastoma and clinical outcomes. BMC Cancer. 2015; 15:514. [PubMed: 26159519]
15. Qin J, et al. The polycomb group protein L3mbtl2 assembles an atypical PRC1-family complex that is essential in pluripotent stem cells and early development. Cell Stem Cell. 2012; 11:319–332. [PubMed: 22770845]
16. Stielow C, et al. SUMOylation of the polycomb group protein L3MBTL2 facilitates repression of its target genes. Nucleic Acids Res. 2014; 42:3044–3058. [PubMed: 24369422]
17. Trojer P, et al. L3MBTL2 protein acts in concert with PcG protein-mediated monoubiquitination of H2A to establish a repressive chromatin structure. Mol Cell. 2011; 42:438–450. [PubMed: 21596310]
18. Yoo JY, et al. Histone deacetylase 3 is selectively involved in L3MBTL2-mediated transcriptional repression. FEBS Lett. 2010; 584:2225–2230. [PubMed: 20385135]
19. Ogawa H, Ishiguro K-i, Gaubatz S, Livingston DM, Nakatani Y. A Complex with Chromatin Modifiers That Occupies E2F- and Myc-Responsive Genes in G₀ Cells. Science. 2002; 296:1132–1136. [PubMed: 12004135]
20. Gao Z, et al. PCGF homologs, CBX proteins, and RYBP define functionally distinct PRC1 family complexes. Mol Cell. 2012; 45:344–356. [PubMed: 22325352]
21. Guo Y, et al. Methylation-state-specific recognition of histones by the MBT repeat protein L3MBTL2. Nucleic Acids Res. 2009; 37:2204–2210. [PubMed: 19233876]
22. Acs K, et al. The AAA-ATPase VCP/p97 promotes 53BP1 recruitment by removing L3MBTL1 from DNA double-strand breaks. Nat Struct Mol Biol. 2011; 18:1345–1350. [PubMed: 22120668]
23. Soutoglou E, et al. Positional stability of single double-strand breaks in mammalian cells. Nat Cell Biol. 2007; 9:675–682. [PubMed: 17486118]
24. Rogakou EP, Boon C, Redon C, Bonner WM. Megabase chromatin domains involved in DNA double-strand breaks in vivo. J Cell Biol. 1999; 146:905–916. [PubMed: 10477747]
25. Lou Z, Minter-Dykhouse K, Wu X, Chen J. MDC1 is coupled to activated CHK2 in mammalian DNA damage response pathways. Nature. 2003; 421:957–961. [PubMed: 12607004]
26. Rodriguez M, Yu X, Chen J, Songyang Z. Phosphopeptide binding specificities of BRCA1 COOH-terminal (BRCT) domains. J Biol Chem. 2003; 278:52914–52918. [PubMed: 14578343]
27. Yu X, Chini CC, He M, Mer G, Chen J. The BRCT domain is a phospho-protein binding domain. Science. 2003; 302:639–642. [PubMed: 14576433]
28. Liu J, et al. Structural mechanism of the phosphorylation-dependent dimerization of the MDC1 forkhead-associated domain. Nucleic Acids Res. 2012; 40:3898–3912. [PubMed: 22234877]
29. Wu H-H, Wu P-Y, Huang K-F, Kao Y-Y, Tsai M-D. Structural Delineation of MDC1-FHA Domain Binding with CHK2-pThr68. Biochemistry. 2012; 51:575–577. [PubMed: 22211259]
30. Stucki M, et al. MDC1 Directly Binds Phosphorylated Histone H2AX to Regulate Cellular Responses to DNA Double-Strand Breaks. Cell. 2005; 123:1213–1226. [PubMed: 16377563]
31. Lou Z, et al. MDC1 maintains genomic stability by participating in the amplification of ATM-dependent DNA damage signals. Mol Cell. 2006; 21:187–200. [PubMed: 16427009]
32. Bekker-Jensen S, Mailand N. The ubiquitin- and SUMO-dependent signaling response to DNA double-strand breaks. FEBS letters. 2011; 585:2914–2919. [PubMed: 21664912]
33. Gurvich N, et al. L3MBTL1 polycomb protein, a candidate tumor suppressor in del(20q12) myeloid disorders, is essential for genome stability. Proc Natl Acad Sci U S A. 2010; 107:22552–22557. [PubMed: 21149733]

34. Schwertman P, Bekker-Jensen S, Mailand N. Regulation of DNA double-strand break repair by ubiquitin and ubiquitin-like modifiers. Nature reviews. Molecular cell biology. 2016; 17:379–394. [PubMed: 27211488]
35. Liu C, et al. RNF168 forms a functional complex with RAD6 during the DNA damage response. J Cell Sci. 2013; 126:2042–2051. [PubMed: 23525009]
36. Panier S, et al. Tandem Protein Interaction Modules Organize the Ubiquitin-Dependent Response to DNA Double-Strand Breaks. Mol Cell. 2012; 47:383–395. [PubMed: 22742833]
37. Penengo L, et al. Crystal structure of the ubiquitin binding domains of rabex-5 reveals two modes of interaction with ubiquitin. Cell. 2006; 124:1183–1195. [PubMed: 16499958]
38. Thorslund T, et al. Histone H1 couples initiation and amplification of ubiquitin signalling after DNA damage. Nature. 2015; 527:389–393. [PubMed: 26503038]
39. Cao J, Yan Q. Histone ubiquitination and deubiquitination in transcription, DNA damage response, and cancer. Front Oncol. 2012; 2:26. [PubMed: 22649782]
40. Hornbeck PV, et al. PhosphoSitePlus, 2014: mutations, PTMs and recalibrations. Nucleic Acids Res. 2015; 43:D512–520. [PubMed: 25514926]
41. Wang Z, et al. USP51 deubiquitylates H2AK13,15ub and regulates DNA damage response. Genes Dev. 2016; 30:946–959. [PubMed: 27083998]
42. Ramachandran S, et al. The RNF8/RNF168 ubiquitin ligase cascade facilitates class switch recombination. Proceedings of the National Academy of Sciences. 2010; 107:809–814.
43. Peuscher MH, Jacobs JJ. DNA-damage response and repair activities at uncapped telomeres depend on RNF8. Nat Cell Biol. 2011; 13:1139–1145. [PubMed: 21857671]
44. Strickfaden H, et al. Poly(ADP-ribosyl)ation-dependent transient chromatin decondensation and histone displacement following laser micro-irradiation. Journal of Biological Chemistry. 2015
45. Deng Y, Guo X, Ferguson DO, Chang S. Multiple roles for MRE11 at uncapped telomeres. Nature. 2009; 460:914–918. [PubMed: 19633651]
46. Lou Z, Chini CCS, Minter-Dykhouse K, Chen J. Mediator of DNA damage checkpoint protein 1 regulates BRCA1 localization and phosphorylation in DNA damage checkpoint control. Journal of Biological Chemistry. 2003; 278:13599–13602. [PubMed: 12611903]
47. Deng M, et al. Deubiquitination and Activation of AMPK by USP10. Mol Cell. 2016; 61:614–624. [PubMed: 26876938]
48. Hamada M, et al. Ran-dependent docking of importin-β to RanBP2/Nup358 filaments is essential for protein import and cell viability. J Cell Biol. 2011; 194:597–612. [PubMed: 21859863]
49. Sanjana NE, Shalem O, Zhang F. Improved vectors and genome-wide libraries for CRISPR screening. Nat Methods. 2014; 11:783–784. [PubMed: 25075903]
50. Pei H, et al. The histone methyltransferase MMSET regulates class switch recombination. J Immunol. 2013; 190:756–763. [PubMed: 23241889]
51. van Steensel B, Smogorzewska A, de Lange T. TRF2 protects human telomeres from end-to-end fusions. Cell. 1998; 92:401–413. [PubMed: 9476899]

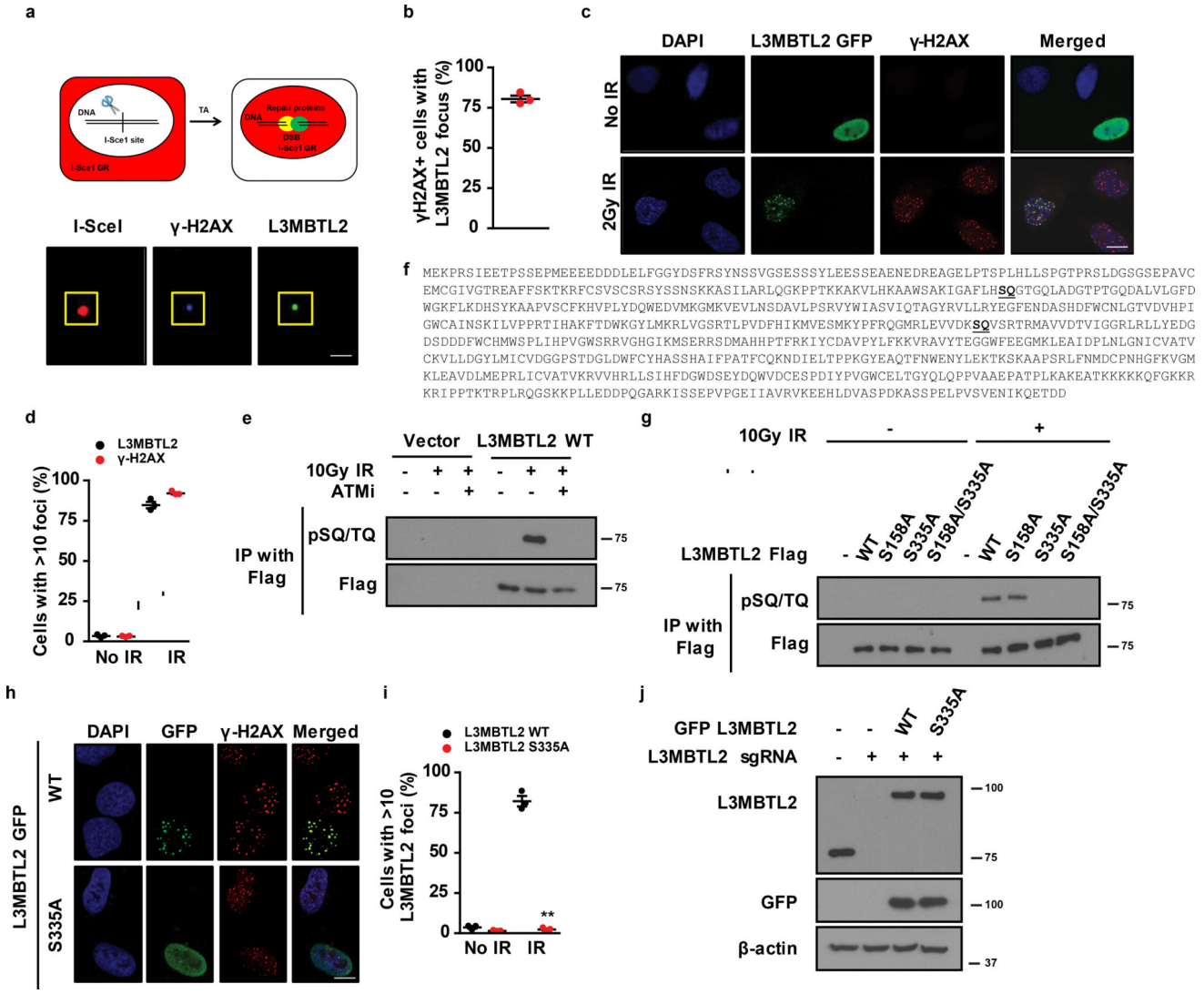

Figure 1. ATM-mediated phosphorylation of L3MBTL2 recruits it to the double strand break site

(**a–b**) L3MBTL2 localizes to the DSB site in U2OS I-SceI cells where one DSB is induced per cell using triamcoline acetonide (red). This L3MBTL2 focus (green) overlaps with γH2AX (blue). The yellow box locates the size of the cut. Inset, schema of the U2OS I-SceI reporter system. (**b**) Quantification of U2OS I-SceI cells with both H2AX and L3MBTL2 foci. (**c–d**) L3MBTL2 forms radiation-induced puncta that overlaps with γ-H2AX in U2OS cells. (**d**) Quantification of the indicated foci with and without irradiation in U2OS cells. (**e–g**) ATM phosphorylates L3MBTL2 at the S335 residue following DNA damage. ATM inhibitor (ATMi) KU55933 was used as control. Protein sequence of L3MBTL2 is shown in **f**. Putative ATM phosphorylation sites are underlined and bolded. (**h–j**) Phosphorylation of L3MBTL2 is required for recruitment of L3MBTL2 to double strand break sites in U2OS cells. Mutation of the phosphorylation site on L3MBTL2 abrogates its localization to DSB sites. U2OS cells in which endogenous L3MBTL2 had been knocked out were transfected with the indicated GFP-tagged plasmids. Cells were exposed to 2GY IR and stained for γ-

H2AX foci (red). Nucleus is stained with DAPI (blue). (**i**) Quantification of L3MBTL2 foci in U2OS cells expressing the indicated plasmids with and without irradiation. Data are represented as the mean ± SEM of n = 3 independent experiments. Circles depict individual data points. Statistical significance was calculated using 2-way ANOVA. **p= 0.000000005 for L3MBTL2 WT vs S335A with IR treatment. Source data are provided in Supplementary Table 1. (**j**) Expression level of the L3MBTL2 constructs in L3MBTL2 knockout and control U2OS cells. L3MBTL2 was knocked out in U2OS cells using CRISPR. GFP-tagged WT or S335A mutant of L3MBTL2 was transfected into these cells. Shown is the comparable expression level of L3MBTL2 in these cells. Representative images of three independent experiments are shown in **a**, **c** and **h**. Scale bars, 10 μm. Representative western blots in **e**, **g**, and **j** are provided from 3 biologically independent experiments. Unprocessed blots are provided in Supplementary Figure 5.

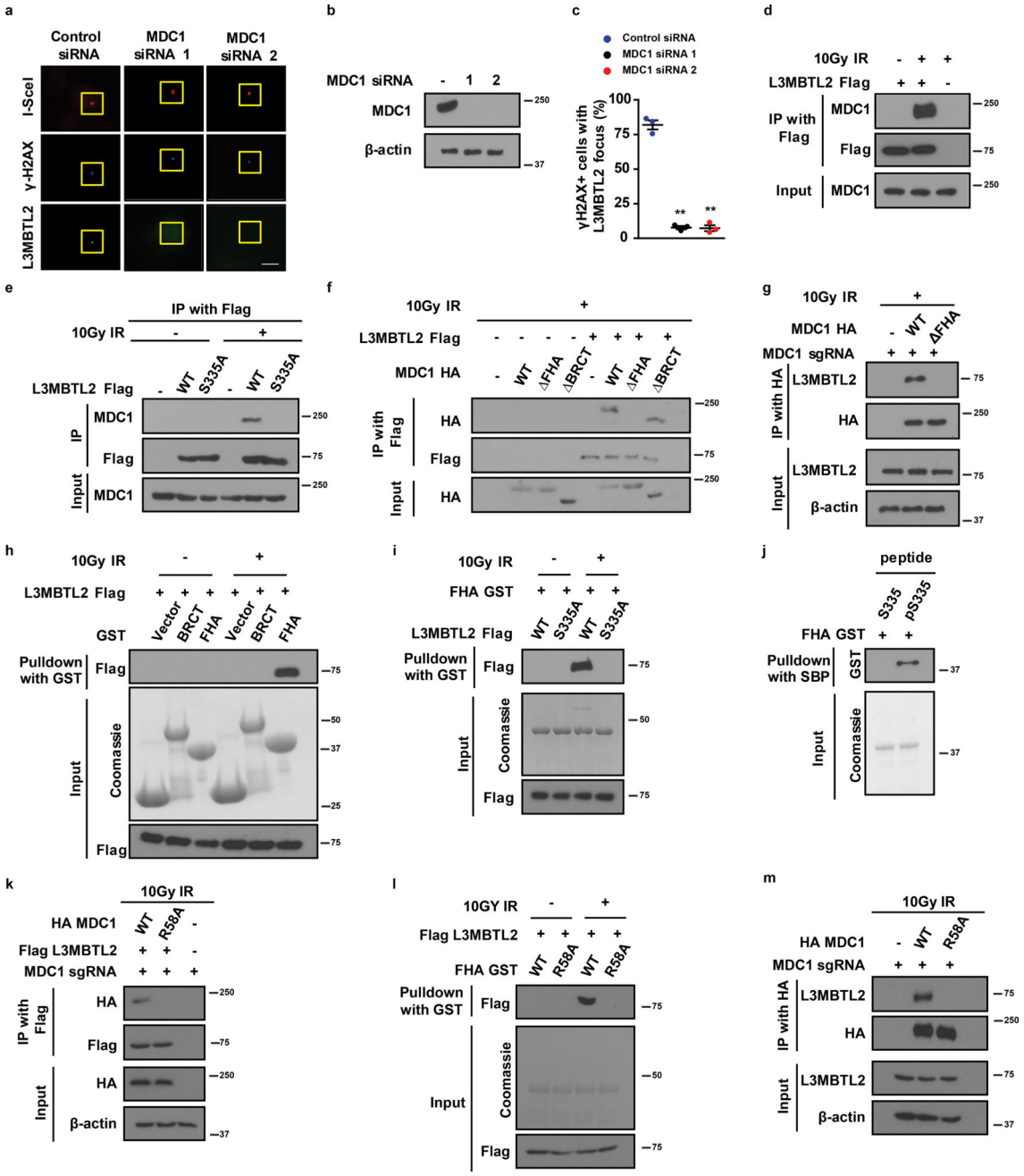

Figure 2. ATM-mediated phosphorylation of L3MBTL2 promotes its interaction with MDC1 and recruits it to the double strand break site

(**a–c**) MDC1 is required for L3MBTL2 recruitment to the DSB site. (**a**) Knockdown of MDC1 using siRNA inhibits L3MBTL2 (green) accumulation at DSB site in U2OS I-SceI cells. γ-H2AX (blue) was used as a positive control. The yellow box locates the site of the cut. (**b**) Knockdown efficiency of MDC1 with siRNA. (**c**) Quantification of U2OS I-SceI cells with L3MBTL2 foci with and without MDC1 knockdown using siRNA. Data are represented as the mean ± SEM of n= 3 independent experiments. Circles depict individual data points. Statistical significance was calculated using 1-way ANOVA. **p= 0.000002 for

control siRNA vs MDC1 siRNA 1 and 2. (**d**) L3MBTL2 interacts with MDC1 following DNA damage. (**e**) DNA damage-induced phosphorylation of L3MBTL2 at S335 is required for its interaction with MDC1. (**f**) L3MBTL2 interacts with the FHA domain of MDC1 upon DNA damage. Deletion of the FHA domain (ΔFHA) abrogates the interaction between MDC1 and L3MBTL2. (**g**) The FHA domain of MDC1 is required for the interaction between MDC1 and L3MBTL2. (**h**) L3MBTL2 interacts with the FHA domain of MDC1 *in vitro*. GST-tagged constructs of MDC1 were incubated with lysates from cells expressing L3MBTL2 and treated with or without radiation. (**i**) L3MBTL2 interacts with the FHA domain of MDC1 *in vitro* following DNA damage. GST-tagged FHA domain of MDC1 was incubated with lysates from L3MBTL2 knockout cells expressing WT or phosphorylation mutant of L3MBTL2 (S335A) and treated with or without radiation. (**j**) The FHA domain of MDC1 directly interacts with phosphorylated L3MBTL2. The indicated peptides of L3MBTL2 (control and pS335) were incubated with GST-tagged FHA domain of MDC1. (**k–m**) Mutation in the FHA domain of MDC1 abrogates the interaction between MDC1 and L3MBTL2 both *in vitro* and *in vivo*. Representative images of three independent experiments are shown in **a**. Scale bars, 10 μm. Representative western blots in **b**, **d**–**m** are provided from 3 biologically independent experiments. Source data and unprocessed blots are provided in Supplementary Table 1 and Supplementary Figure 5, respectively.

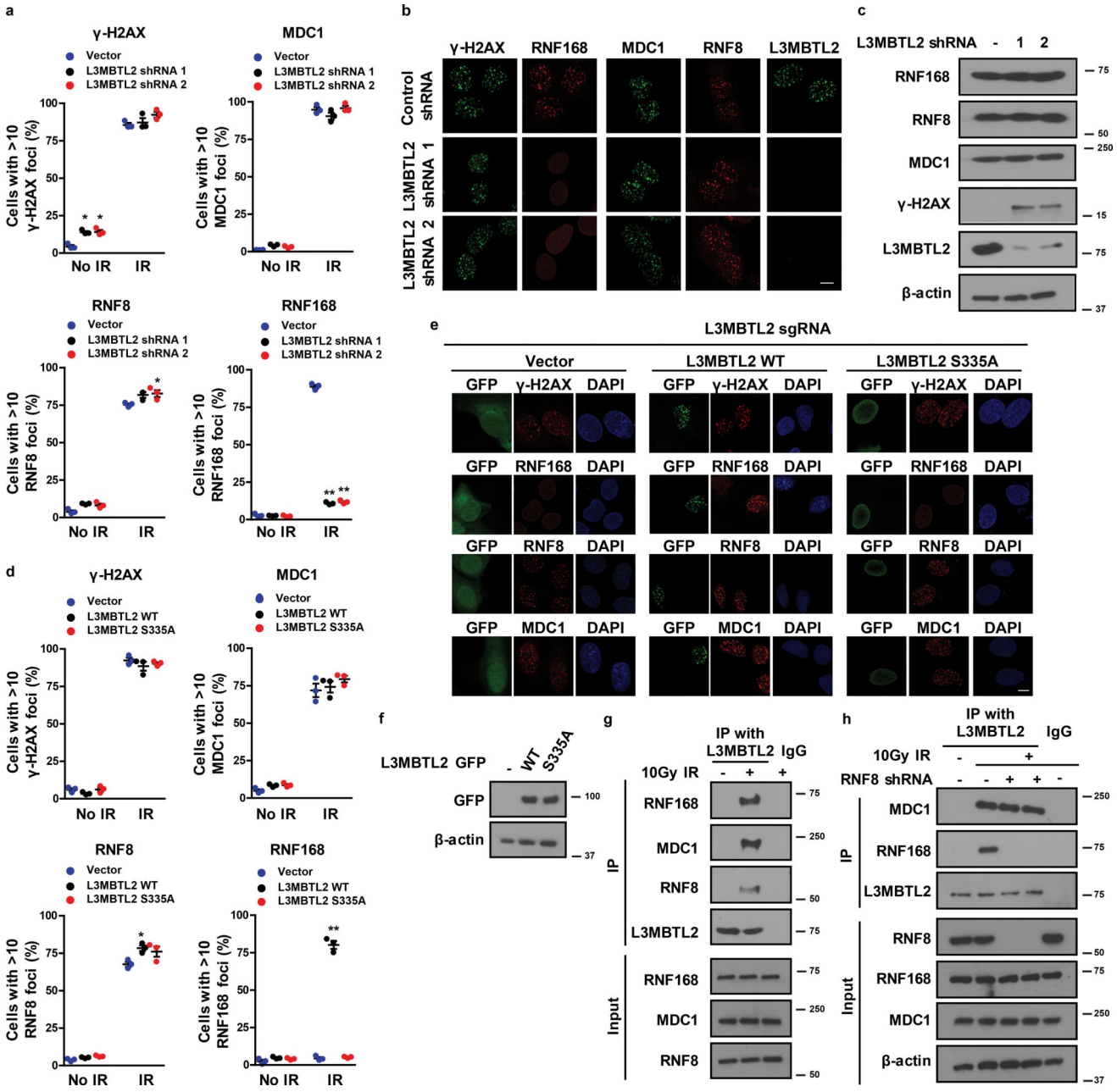

Figure 3. L3MBTL2 recruits RNF168 to the double strand break site

(**a–c**) shRNA mediated knockdown of L3MBTL2 in U2OS cells prevents formation of RNF168 foci following DNA damage. Shown are (**a**) quantification and (**b**) representative images of cells with γ-H2AX, MDC1, RNF8, and RNF168 foci after 2GY irradiation. (**c**) Knockdown of L3MBTL2 using shRNA does not affect RNF168 protein level in U2OS cells. (**d–f**) Phosphorylation of L3MBTL2 is required for RNF168 foci formation following DNA damage. Shown are (**d**) quantification and (**e**) representative of γ-H2AX, MDC1, RNF8, and RNF168 foci after 2GY irradiation in L3MBTL2 knockout U2OS cells expressing wild-type (WT) or the phosphorylation mutant of L3MBTL2 (S335A). (**f**) Western blot showing the expression level of WT and S335A mutant of L3MBTL2. (**g**)

MDC1, RNF8 and RNF168 interact with endogenous L3MBTL2 following DNA damage. Cells were exposed to the indicated doses of irradiation. Lysates were collected after an hour and proteins interacting with L3MBTL2 were assessed. (**h**) DNA damage-induced interaction between RNF168 and L3MBTL2 is dependent on RNF8. Knockdown of RNF8 using shRNA does not affect the interaction between endogenous MDC1 and L3MBTL2. Cells were exposed to the indicated doses of irradiation. Lysates were collected after an hour and proteins interacting with L3MBTL2 were assessed. Data in **a** and **d** are represented as the mean ± SEM of n = 3 independent experiments. Circles depict individual data points. Statistical significance was calculated using 2-way ANOVA. *p<0.05, **p<0.01 (vector vs all other groups). Please refer to Supplementary Table 1 for exact p values in **a** and **d**. The experiments in **b** and **e** were repeated 3 independent times with similar results. Representative western blots in **c** and **f** to **h** are provided from 3 biologically independent experiments. Scale bars, 10 μm. Source data and unprocessed blots are provided in Supplementary Table 1 and Supplementary Figure 5, respectively.

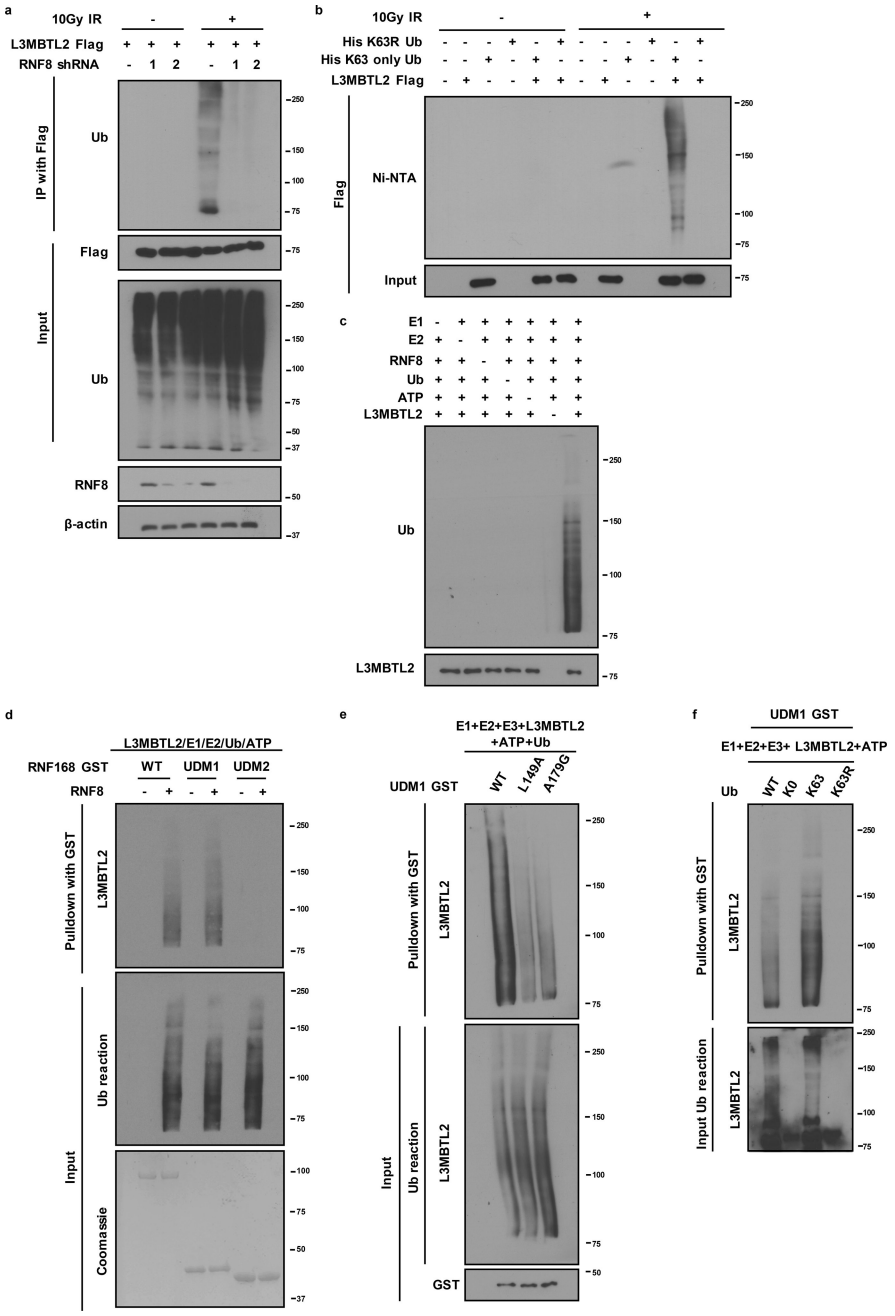

Figure 4. RNF8 mediated K63 linked ubiquitylation of L3MBTL2 following DNA damage is critical for the interaction with UDM1 of RNF168 and subsequent histone ubiquitylation

(**a–b**) RNF8 ubiquitylates L3MBTL2 following DNA damage and forms K63 linkage. (**a**) RNF8 was knocked down using shRNA in MDA-MB-231 cells expressing L3MBTL2. Cells were subjected to control or 10GY irradiation. Lysates were collected after 1 hr. The interaction between the indicated proteins was analyzed. Blots were probed with the indicated antibodies. (**b**) MDA-MB-231 cells were transfected with the indicated constructs. Cells were exposed to the indicated doses of radiation and lysed after an hour. Immunoprecipitation was performed using nickel (His) beads. Blots were probed with the

indicated antibodies. (**c**) RNF8 ubiquitylates L3MBTL2 *in vitro*. The indicated recombinant proteins along with their required cofactors were incubated at 30°C for 1 hour. The reaction was analyzed by western blot. Blots were probed with the indicated antibodies. (**d**) L3MBTL2 interacts with recombinant UDM1 domain of RNF168 *in vitro* in an RNF8 dependent manner. The indicated GST-tagged constructs of RNF168 were incubated with the reaction product of (**c**) with and without RNF8 for an hour. The result was analyzed by western blot and blots were probed with the indicated antibodies. (**e**) Mutations in UDM1 domain of RNF168 reduces its interaction with L3MBTL2. The reaction product from (**c**) was incubated with the indicated GST-tagged UDM1 constructs for an hour. The result was analyzed by western blot and blots were probed with the indicated antibodies. (**f**) L3MBTL2 interacts with UDM1 via K63-linked ubiquitin chains. The indicated recombinant proteins (without UDM1 GST) along with required cofactors were incubated at 30°C for 1 hour. The reaction product was incubated with GST-tagged UDM1 construct for an hour. The reaction was analyzed by western blot. Blots were probed with the indicated antibodies. Representative western blots are provided from 3 biologically independent experiments in **a** to **f**. Unprocessed blots are provided in Supplementary Figure 5.

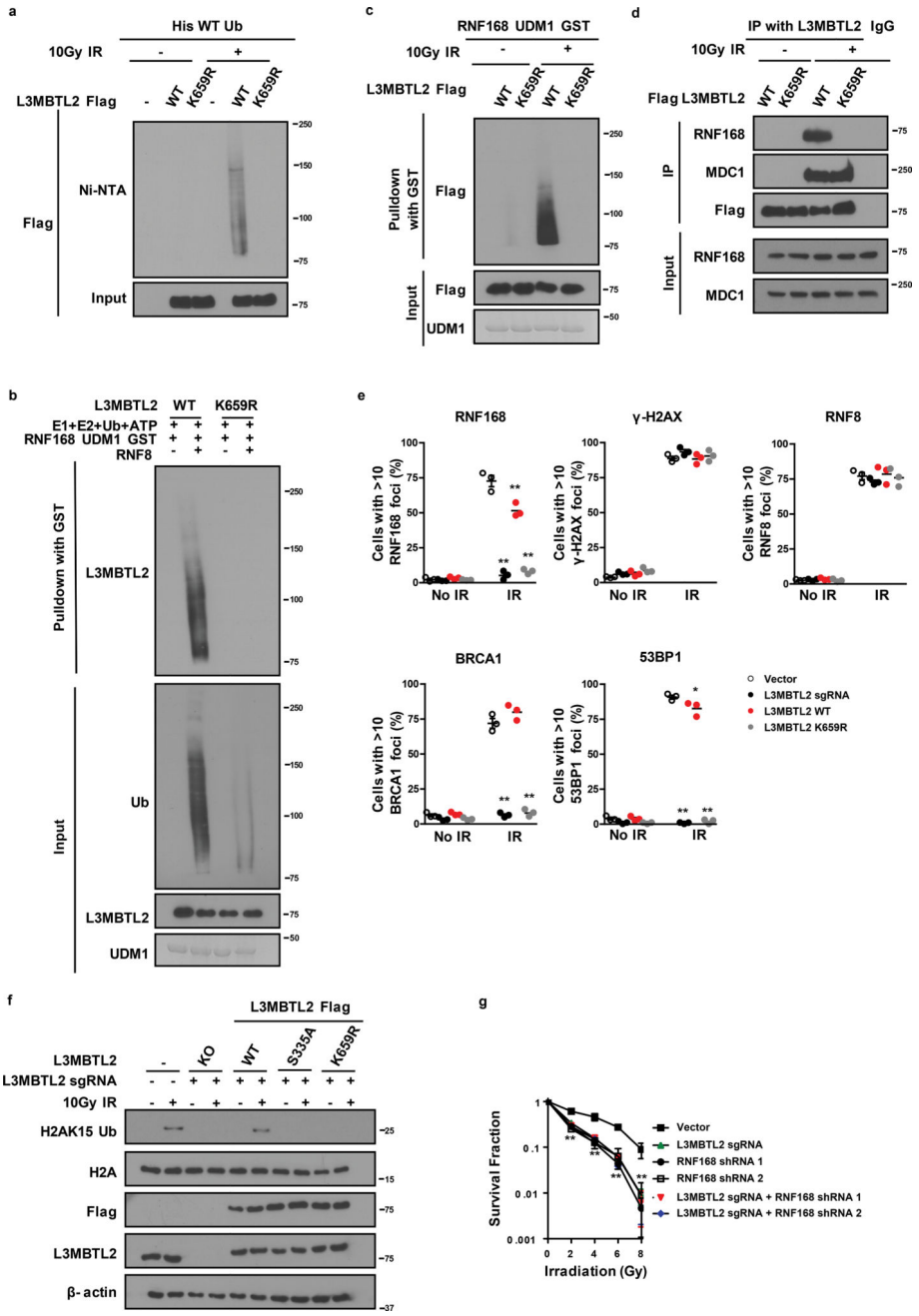

Figure 5. DNA damage induced RNF8 mediated ubiquitylation of L3MBTL2 is critical for DNA DSB repair

(**a**) L3MBTL2 is ubiquitylated at K659 following DNA damage. The indicated plasmids and His-tagged wild-type ubiquitin (His WT Ub) were transfected into L3MBTL2 knockout cells. Lysates were acquired an hour following 10GY irradiation and subjected to immunoprecipitation. (**b**) RNF8 is required for the interaction between the UDM1 domain of RNF168 and L3MBTL2 *in vitro*. The indicated recombinant proteins were incubated with L3MBTL2 purified from L3MBTL2 knockout cells expressing the indicated plasmids. Immunoprecipitation was performed with GST-tagged UDM1 protein. (**c**) Ubiquitylation of

L3MBTL2 is required for its binding with recombinant UDM1 domain of RNF168 *in vitro*. L3MBTL2 knockout cells expressing the indicated L3MBTL2 constructs were exposed to the indicated doses of irradiation, lysed after an hour. L3MBTL2 was purified from these lysates and incubated with GST-tagged UDM1 domain of RNF168 for an hour. (**d**) Ubiquitylation is important for the interaction between RNF168 and L3MBTL2 but not MDC1. (**e**) The ubiquitylation mutant (K659R) fails to form radiation-induced RNF168 foci. (**f**) Analysis of irradiation induced H2A ubiquitylation by RNF168 in chromatin fraction of L3MBTL2 knockout cells expressing the indicated plasmids. (**g**) Loss of L3MBTL2 sensitizes cells to irradiation. Survival assays of L3MBTL2 knockout MDA-MB-231 cells treated as indicated and exposed to the indicated doses of irradiation. Data are represented as the mean ± SEM of n = 3 independent experiments in **e** and **g**. Circles depict individual data points. Statistical significance was calculated using 2-way ANOVA. *p<0.05, **p<0.01 (vector vs all other groups) in **e**. Please refer to Supplementary Table 1 for exact p values. p=0.0001 for vector vs all other groups at each time point in **g**. Representative western blots are provided from 3 biologically independent experiments in **a–d** and **f**. Source data and unprocessed blots are provided in Supplementary Table 1 and Supplementary Figure 5, respectively.

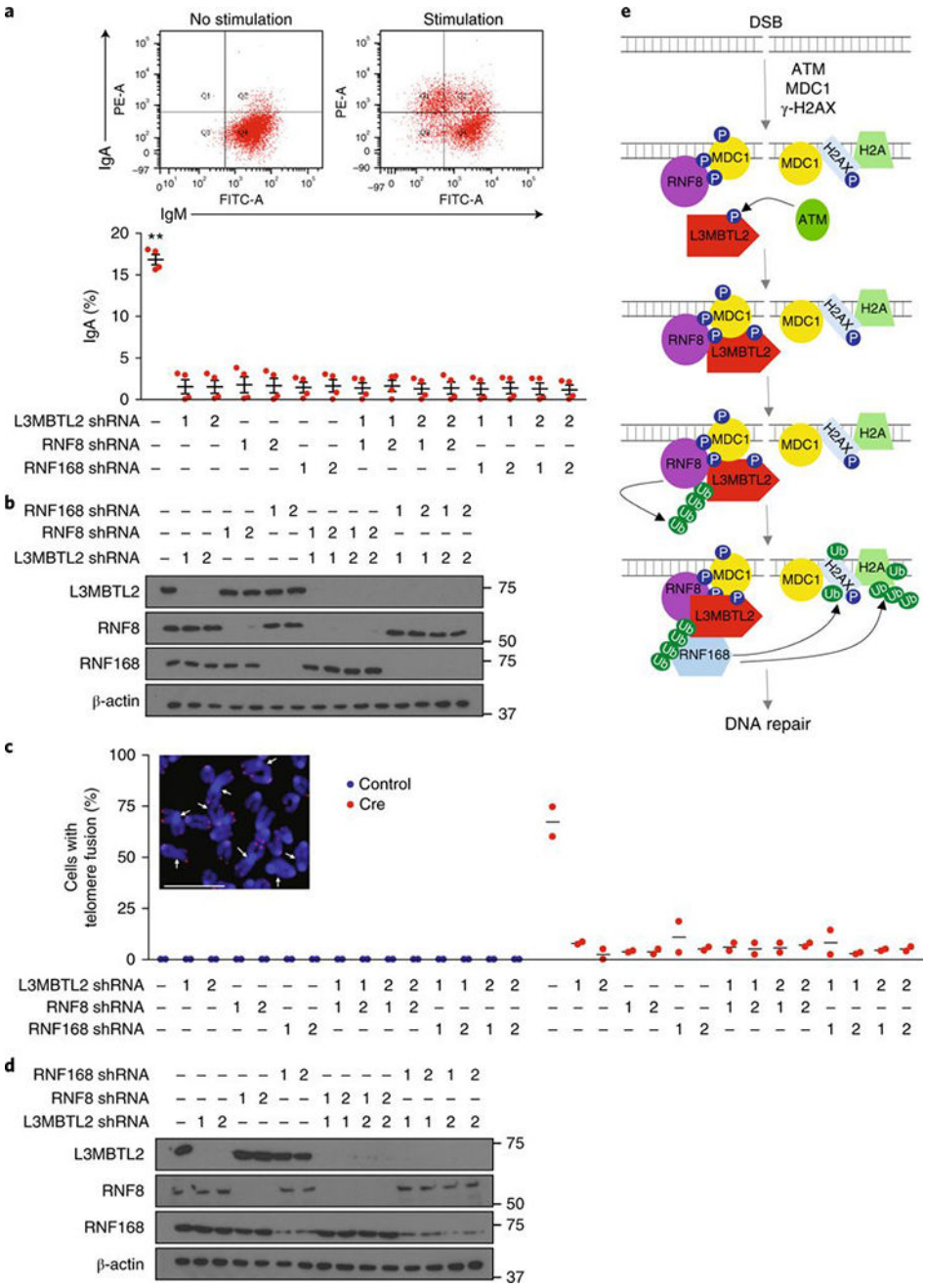

Figure 6. L3MBTL2 induces class switch recombination and chromosome end fusion

(**a–b**) L3MBTL2 is required for class switch recombination. CH12F3-2a cells were treated as indicated. Class switch recombination was stimulated using ligand. IgM to IgA conversion was assessed by immunostaining followed by flow cytometry. Inset is shown a representative image of IgM to IgA conversion with treatment. (**b**) Representative western blot showing the knockdown efficiencies of shRNAs. (**c–d**) L3MBTL2 is required for telomere fusion. $TRF2^{F/F}$ MEFs were treated as indicated. Cells were infected with Cre lentivirus, treated with KaryoMAX Colcemid, fixed, and stained with PNA FISH. Percent of cells with telomere fusion was assessed. Inset is shown a representative image of telomere

fusion (white arrows). DNA was stained with DAPI (blue). (**d**) Representative western blot showing the knockdown efficiencies of shRNAs. (**e**) Model for RNF8, L3MBTL2 and RNF168 function in ubiquitin dependent signaling after DNA DSBs. We propose that ATM-mediated phosphorylation of L3MBTL2 promotes its interaction with MDC1 and recruits it to the DSB site. It is subsequently ubiquitylated by RNF8 which recruits RNF168 to the damage site. RNF168, in turn, monoubiquitylates H2A-type histones to amplify the DNA damage response and recruit downstream DNA repair proteins for proper DSB signaling. Data are represented as the mean ± SEM of n = 4 independent experiments for (**a**). In (**c**) data from two independent experiments are shown with a line indicating the mean. Circles depict individual data points. Scale bars, 10 μm. Statistical significance was calculated using 1-way ANOVA in **a** ($p=0.0001$ for all groups vs control shRNA). Representative western blots in **b** and **d** are from 4 and 2 biologically independent experiments, respectively. Source data and unprocessed blots are provided in Supplementary Table 1 and Supplementary Figure 5, respectively.